Advanced Materials Research *Online: 2014-08-11*
ISSN: 1662-8985, Vol. 996, pp 88-93
doi:10.4028/www.scientific.net/AMR.996.88

Effect of interlamellar spacing on the monotonic behavior of C70 pearlitic steel

Houda Yahyaoui[ab]; Habib Sidhom[a]; Chedly Braham[b]; Andrzej Baczmanski[c]; Manuel Francois[d]; Wilfrid Seiler[b]

[a] Mechanical, Materials and Processes Laboratory (LR99ES05), ESSTT, 5, Avenue Taha Hussein 1008, University of Tunis, Tunisia.
[b]Laboratoire Procédés et Ingénierie en Mécanique et Matériaux (PIMM, CNRS UMR 8006), ENSAM, 151 Bd de l'Hôpital, 75013 Paris, France.
[c]AGH-University of Science and Technology, Faculty of Physics and Applied Computer Science, Al. Mickiewicza 30, 30-059 Kraków, Poland.
[d]Université de Technologie de Troyes (UTT), 12 rue Marie Curie, 10010 Troyes, France

yahyaoui_houda08@yahoo.fr[a], habib.sidhom@gmail.com[a], chedly.braham@paris.ensam.fr[b], Andrzej.Baczmanski@fis.agh.edu.pl[c], manuel.francois@utt.fr[d]

Keywords: Pearlitic steel, X-ray diffraction, Synchrotron radiation, Self-consistent model, Critical shear stress, Lattice strains.

Abstract The effect of interlamellar spacing on monotonic behavior of C70 pearlitic steel was investigated. Tensile tests under X-ray diffraction coupled with self-consistent model have been used to identify the role of interlamellar spacing on the ferrite plasticity parameters and residual stresses. It has been established that yielding of pearlite is controlled by ferrite critical shear stresses ($\tau_c^0(\alpha)$) which is higher for the smallest interlamellar spacing. Moreover, the residual stress level in ferrite is higher for the largest interlamellar spacing under the same imposed total strain. Lattice strains, measured by synchrotron X-ray diffraction, show elastic and plastic anisotropy of ferrite crystallites and high stresses in cementite which confirm the self consistent model calculation.

Introduction

Pearlitic carbon steels are recommended for automotive components manufacturing such as suspension cables, engineering springs. Low cost, high strength, wear resistance and high fatigue life are their main advantages as shown by earlier [1]. Nevertheless, the behavior of these materials is very sensitive to the microstructure characteristics like cementite volume fraction, interlamellar spacing, pearlitic colonies and early austenitic grain size. The effect of microstructure has been discussed on the basis of load partitioning between ferrite and cementite phases assessed by « in-situ » tensile tests under X-ray [2, 3], synchrotron [2-4] and neutron diffraction [5, 6]. It has been established that for the fully pearlitic structures, the load partitioning is mainly controlled by cementite shape and the interlamellar spacing. Hyzak and Bernstein [7] showed that the strength of fully pearlitic steel is controlled primarily by the interlamellar spacing, while the toughness is strongly dependent on the prior-austenitic grain size.

At the phase scale, it has been established that the microstructure parameters control the stress, strain and damage distribution in ferrite and cementite phases resulting from load transfer modes. Shinozaki et al. [8] reported that the local stress in the constituent phase is increased with decreasing interlamellar spacing. This effect of microstructures controls the loading partitioning between ferrite and cementite phases which is characterized by a specific behavior under monotonic [2] and cyclic loading [9]. Several studies have used self-consistent models [2, 3, 10] to identify the behavior of pearlitic steels at macroscopic and microscopic scales under monotonic [3, 5] and cyclic

[11] loading. Nevertheless, little work has been published on the effect of interlamellar spacing on the plasticity parameters and residual stress of pearlitic steel constituents. For these reasons, X-ray diffraction coupled with self-consistent model are used in this work to identify the role of the interlamellar spacing of C70 fully pearlitic steel on the ferrite strength, the ferrite plasticity parameters and the residual stress induced by plasticity. The lattice strain evolution in ferrite and cementite are measured during "in situ" tensile test using high energy X-ray diffraction.

Material and heat treatments

The pearlitic steel EN C70 (SAE 1070), studied in this work, was provided by ASCOMETAL France company in the form of cylindrical bars of 80 mm in diameter obtained by hot rolling. The chemical composition of this steel is given in Table 1. Two annealing treatments have been selected to provide two different pearlitic microstructure configurations (Fig. 1). Table 2 summarizes the annealing treatment conditions and the resulting microstructure characteristics.

Table 1. Chemical composition of C70 pearltic steel (wt %)

C	Si	Mn	S	P	Ni	Cr	Mo	Cu	Al	Fe
0.68	0.192	0.846	0.010	0.010	0.114	0.160	0.027	0.205	0.042	Balance

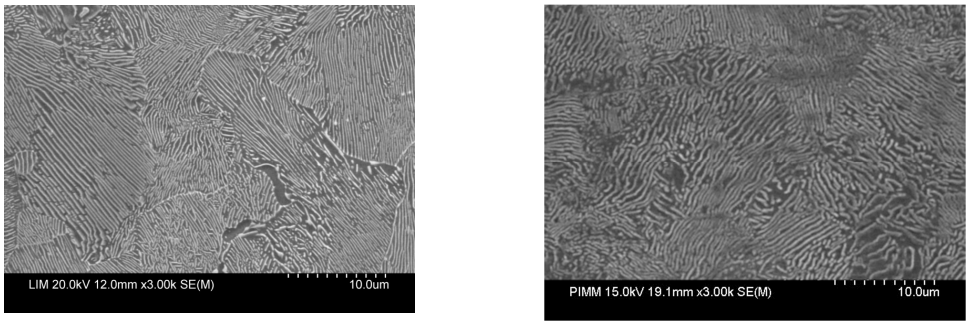

Fig. 1 Microstructures of C70 pearlitic steel: (a) C70 (HT1); (b) C70 (HT2).

Table 2. Heat treatments, metallurgical characteristics and mechanical properties of the two microstructures

Annealing treatment	Colonies size [µm]	Grains size [µm]	Interlamellar Spacing Sp [nm]	Yield stress [MPa]	Ultimate tensile strength [MPa]	Elongation (%)	Hardness HV_{50}
HT1: Austenizing at 1073 K for 0.5 h followed by cooling under calm air	7.4	19	230	396	875	17	220±10
HT2: Austenizing at 1323 K for 0.11 h followed by cooling under blowing air	7.9	26	170	498	997	15	270±15

Experimental setup

The $\sin^2\psi$ X-ray diffraction method was used to determine the ferrite stresses. This method is based on the measurement of peak positions for a given h k l reflection and for various directions of the scattering vector with respect to the sample, described by the ψ and φ angles. Measurements were carried on a Set-X type diffractometer. Chromium radiation (λKα (Cr) = 0.22911 nm) was used for the (2 1 1) reflection of ferrite. The stress in cementite phase was not measured because the diffraction peak intensities from this phase (10% of total pearlitic volume) are very low.

Synchrotron diffraction was used to measure the lattice strains at ID15b beamline (ESRF, Grenoble, France). In situ tensile test were performed with beam size 100x100 µm in transmission mode (average through the sample thickness) with monochromatic 87keV X-ray radiation

(wavelength λ = 0.14256 Å). The diffraction pattern was recorded using a Pixium 2D detector (range 2θ= 1.8° – 7° covers the main reflections from the measured steels) in order to measure lattice strains.

Results and discussion

Effect of interlamellar spacing on the ferrite behavior

The superimposition ferrite stress-imposed strain curves (Fig. 2) reveals the effect of pearlitic microstructure characteristics, resulting from the two annealing treatments of C70 steel, on the tensile behavior of ferritic phase. Indeed, analyzing the stress evolution in ferritic phase it was found that the ferritic intrinsic yield stress for HT2 microstructure is around σ_{11}=280 MPa, which is higher than the ferritic yield stress σ_{11}=210 MPa determined for HT1 microstructure. This difference is mainly attributed to the pearlite microstructure (Sp values) since the initial residual stresses level in ferrite is the same (σ_{res} = -55 MPa for the two microstructures). The difference between the two pearlite phases (ferrite and cementite) behavior under tensile loading is considered to be responsible for the residual stress induced by plasticity. Indeed, X-ray diffraction measurements performed after tensile loading (stress ratio $\frac{\Sigma_{11}}{R_e} \geq 1.1$) followed by total unloading showed a compressive residual stress generated in ferrite. However, the plastic induced compressive residual stresses are higher for the larger interlamellar spacing (Fig. 2).

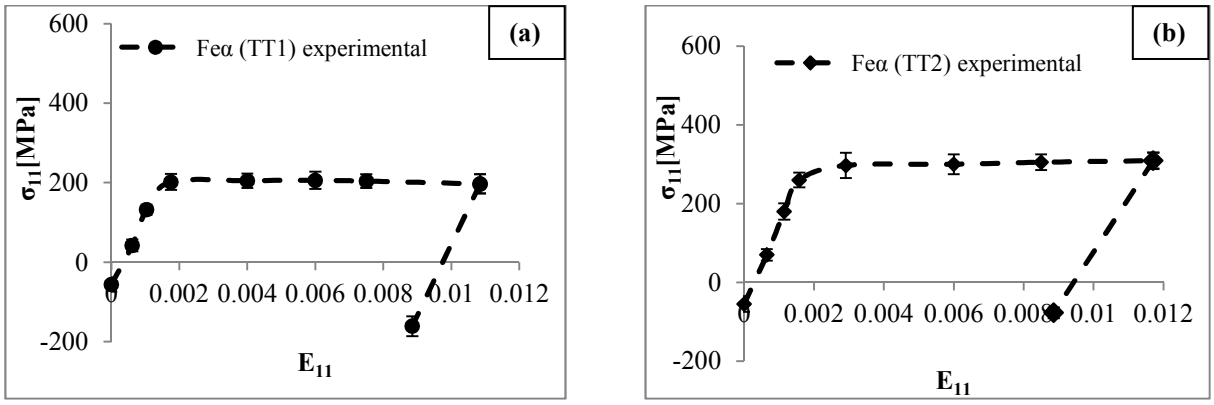

Fig. 2 Evolution of ferrite stress σ_{11} vs. total imposed strain E_{11} measured using laboratory X-ray diffraction during « in-situ » tensile tests: (a) C70: HT1 and (b) C70: HT2.

Modeling results and validation

Self-consistent model formulation

A self-consistent model is used in this study to identify the elastoplastic parameters (critical shear stresses τ_0^c and hardening matrix H) of ferritic phase in the pearlitic steel C70. The self-consistent scheme [12, 13] used for the scale transition and isotropic hardening was assumed, i.e., all elements of the Hst matrix are equal to the same value H. The initial critical shear stress τ_c^0 and the work hardening parameter (H) were determined using the method proposed in the work of Baczmanski and Braham [14].

Model parameters

To predict the elastoplastic behavior of the two pearlitic microstructures, the calculations were performed for 10,000 ellipsoidal inclusions representing grains of cementite (10%) and ferrite (90%). The orientations of axes of cementite inclusion were randomly distributed, while spherical grains were assumed for ferrite. Random orientations distribution of lattice in ferritic grains was assumed. The elastic behaviour of ferrite was characterized by given single crystal elastic constants.

Therefore, isotropic Young's modulus and Poisson's ratio were attributed to the inclusions of cementite (Table 3). Calculations were performed with the assumption that two families of slip systems (i.e. <111>{211} and <111>{110}) are active during the plastic deformation for ferrite. An elastic behavior of cementite was assumed for the whole range of deformation as indicated by the literature data [4, 10, 15]. The initial residual stresses are taken into account in calculations and assumed to be equal for all grains in the same phase.

Table 3. Elastic properties of phases

Phase	C_{11} [GPa]	C_{12} [GPa]	C_{44} [GPa]	G [GPa]	υ	Reference
Ferrite	231.4	134.7	116.4	-	-	[3]
Cementite	-	-	-	90	0.275	[16]

Plasticity parameters

The ferrite plasticity parameters ($\tau_0^c(\alpha)$ and H), for both microstructures, were identified on the basis of the iterative modification of plasticity parameters in calculations that ensure an optimal agreement with experimental data for macroscopic curves (Fig.3) and ferrite behaviour determined by «in-situ» X-ray tensile tests (Fig.4). Such comparison of the macroscopic Σ_{11}-E_{11} plots, shown in Figs. 3a and 3b, reveals a good agreement for the two annealed microstructures. However, a small underestimation of the theoretical macro-stresses can be observed.

We can conclude that the values of plastic parameters obtained by fitting the model on the X-ray data are also underestimated (i.e. the lower bound for $\tau_0^c(\alpha)$ was found, when value of H remains always close to zero). To obtain the upper limit of shear stresses the fitting of model macroscopic curve to the result of mechanical tensile test (Σ_{11}-E_{11} plot) was also done. The limits of the optimal values of the parameters $\tau_0^c(\alpha)$ and H ensuring the good agreement initial critical shear stress τ_c^0 is much higher for the smaller interlamellar spacing of the pearlitic microstructure (HT2) between experimental and theoretical data are given in Table 4.

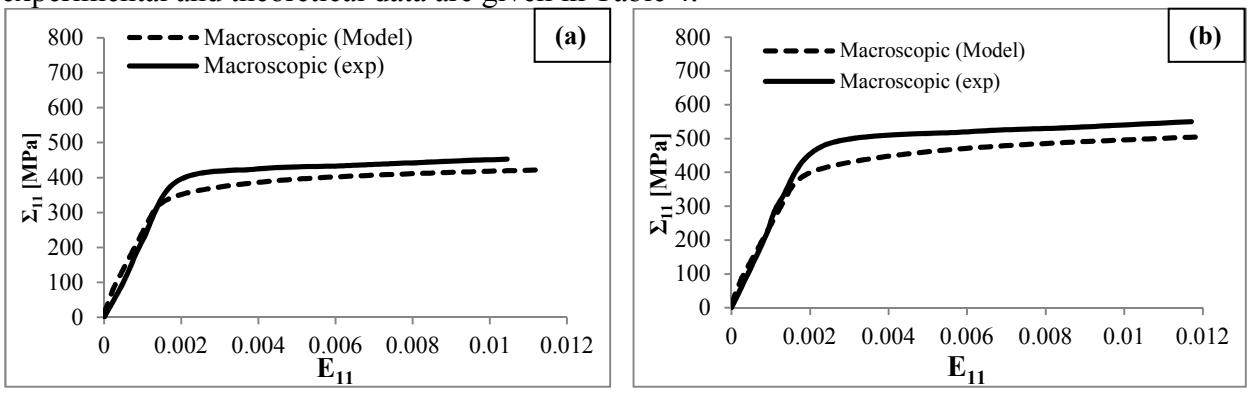

Fig. 3 Results of the mechanical tensile test compared with model prediction (a) C70 TT1; (b) C70 TT2.

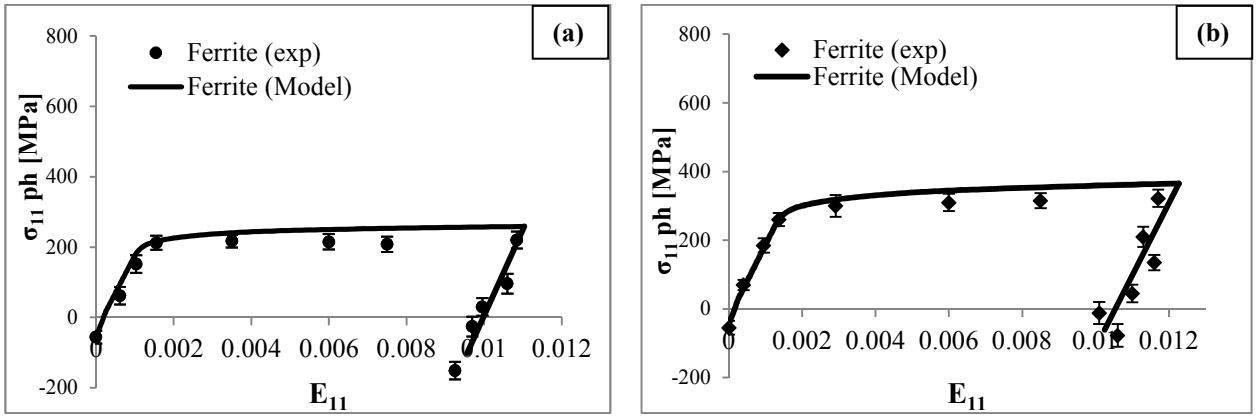

Fig. 4 The results of the « in-situ » tensile test compared with the model prediction (a) C70 TT1; (b) C70 TT2.

Table 4. Ferrite parameters of plasticity identified by self-consistent model

Phase	Structure	τ_c^0 (MPa)	H (MPa)
Ferrite	C70 : HT1	75-86	2
	C70 : HT2	105-120	2
Cementite	C70: HT1/ HT2	Elastic behavior	

Lattice strains

Analyzing the lattice strain vs. applied stress, determined by synchrotron measurements (Fig.5), it can be found that the lattice strain in ferrite increases linearly with applied load in the beginning of the deformation indicating the elastic behavior of ferrite crystals. The values of the slopes of this linear range vary from a direction [hkl] to another reflecting an elastic anisotropy. The end of the linear range marked the beginning of the plasticity of ferrite crystals. In the yield point of ferrite, load is transferred to cementite and tendency of lattice strains evolution changes significantly for both phases. Less load is transferred to the Fe3C phase from [200]Feα direction than from [220]Feα and [211]Feα direction reflecting the plastic anisotropy of ferrite crystallites.

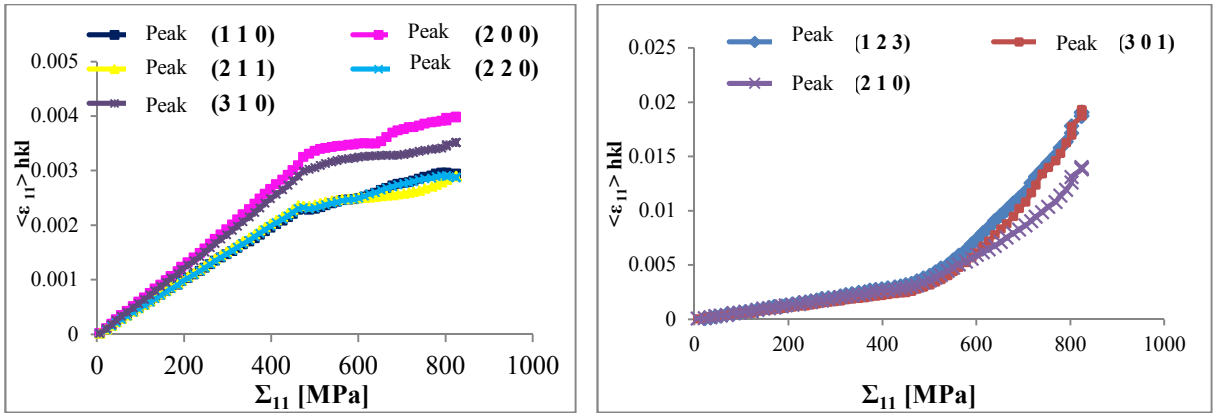

Fig. 5 Elastic lattice strains $< \varepsilon_{11} >$ {hkl} parallel to the load direction, vs applied stress Σ_{11}, measured by synchrotron radiation, for C70 HT2 pearlitic steel.

Summary

In this study, the effect of interlamellar spacing on the ferrite behavior of C70 pearlitic steel was investigated. The main results can be summarized as follow:

- Yielding of ferrite is controlled by the interlamellar spacing: $\sigma_{y(Fe\alpha)}$= 280 MPa for Sp = 170 nm and $\sigma_{y(Fe\alpha)}$ =210 MPa for Sp =230 nm. This result is consistent with the ferrite critical shear stress identified by the self-consistent model: $\tau_c^0(\alpha)$ = 105-120 MPa and $\tau_c^0(\alpha)$ =75-86 MPa for Sp = 170 nm and Sp =230 nm, respectively.
- Plastic deformation of pearlitic steel induces compressive residual stresses in ferrite. Residual stress levels of the two phases are higher for the largest interlamellar spacing.
- Lattice strains evolution show an elastic and plastic anisotropy of ferritic phase as well as high stresses in cementite which confirm the elastic behavior assumption used in self consistent model.

Acknowledgements. We acknowledge the European Synchrotron Radiation Facility for provision of synchrotron radiation facilities and we would like to thank Dr. Thomas Buslaps for assistance in using beamline ID15b.

References

[1] G. Langford, Metall. Trans. A, 8A (1977) 861-875.
[2] M. Belassel, in, ENSAM Paris, 1994.
[3] K. Inal, J. L. Lebrun, M. Belassel, Metall. Mater. Trans., 35A (2004) 2361- 2369.
[4] M. L. Young, J. D. Almer, M. R. Daymond, D. R. Haeffner, D. C. Dunand, Acta Mater., 55 (2007) 1999–2011.
[5] M.R. Daymond, H.G. Priesmeyer, Acta Materialia, 50 (2002) 1613-1626.
[6] Y. Tomota, P. Lukas, D. Neov, S. Harjo, Y. R. Abe, Acta Mater., 51 (2003) 805-817.
[7] J.M. Hyzak, I. Bernstein, Metall. Trans. A, 7A (1976) 1218-1224.
[8] T. Shinozaki, S. Morooka, T. Suzuki, Y. Tomota, T. Kamiyama, in: The 3rd International Conference on Advanced Structural Steels Gyeongju, Korea, 2006.
[9] R.A. Winholtz, J.B Cohen, Metall. Trans, 23 A (1992) 341-354.
[10] C. Schmitt, P. Lipinski, M. Berveiller, I. J. Plasticity., 13 No 3 (1997) 183-199.
[11] X. Long, X. Peng, W. Pi, Acta Mech Sin, 24 (2008) 91–99.
[12] P. Lipinski, M. Berveiller, I. J. Plasticity., 5 (1989) 149-152.
[13] A. Baczmański, P. Zattarin, P. Lipiński, K. Wierzbanowski, Arch. Metall., 45 (2000) 163-184.
[14] A. Baczmanski, C. Braham, Acta Mater., 52 (2004) 1133–1142.
[15] E. C. Oliver, M. R. Daymond, P. J. Withers, Acta Materialia, 52 (2004) 1937–1951.
[16] H. Ledbetter, Materials Science and Engineering, A 527 (2010) 2657–2661.